ORIGINAL PAPER

Ground Control Method of Using Roof Cutting Pressure Release and Energy-Absorbing Reinforcement for Roadway with Extra-Thick Hard Roof

Qi Wang[1,2,3] · Zhenhua Jiang[1,3] · Bei Jiang[1,2] · Manchao He[1] · Jun Yang[1] · Haojie Xue[1,3]

Abstract

Coal mining in the western region of China is often faced with extra-thick coal seams and extra-thick hard roof, where the roof is difficult to collapse in time, resulting in large-suspended area in the gob and the frequent occurrence of dynamic disasters such as mine earthquakes. To this end, we propose an integrated ground control method of roof cutting pressure release and energy-absorbing reinforcement for roadway with hard roof. We take the #122108 working face of the Caojiatan coal mine as the engineering example to apply this new method. The stress reduction rate is used to analyze the pressure relief effect. The influence of pressure relief parameters on the roadway is analyzed through numerical experiments. Three-dimensional stress evolution of the surrounding rock using the optimized parameters is further studied, which verifies the advantages of the new method, as evidenced by the reduction of stress up to 40.87%. Moreover, we conduct physical model test of the new method and reveal the control mechanism on the surrounding rock. The deformation of the roof and floor of roadway with roof cutting is lower than that of the roadway without roof cutting and the maximum deformation is reduced by 52.26%. Subsequently, we design the field roof cutting parameters for pressure release and energy-absorbing reinforcement, and evaluate the parameters of roof cutting, strengthen blasting, and energy-absorbing cables. Field monitored data show that the average deformation of the roadway floor using the new method is 201.8 mm, which is 66.37% smaller than that of roadway without using the new method, and the peak stress at the working face is 27.75% less than that without using the new method. The validity of the physical model test results and the rationality of the design parameters for pressure relief and reinforcement is verified through the field data.

Highlights

- An integrated ground control method of roof cutting pressure release and energy-absorbing reinforcement for roadway with hard roof is proposed.
- The design basis and control mechanism of roof cutting pressure release and energy-absorbing reinforcement parameters for thick hard roof roadway are clarified by numerical and large-scale 3D geological model tests.
- The design and field application of core parameters of directional roof cutting pressure release and energyabsorbing reinforcement have been successfully carried out.

✉ Bei Jiang
jiangbei519@163.com

1 State Key Laboratory for Geo-Mechanics and Deep Underground Engineering, China University of Mining and Technology-Beijing, Beijing 100083, China

2 State Key Laboratory of Explosion Science and Technology, Beijing Institute of Technology, Beijing 100081, China

3 Research Center of Geotechnical and Structural Engineering, Shandong University, Jinan 250061, China

1 Introduction

With the gradual depletion of coal resources in the eastern and central regions of China, coal mining has shifted to the western region. The western region has abundant coal resources with thick coal seams (Bin 2016; Chen et al. 2017; Wei et al. 2022; Wojtecki et al. 2022), which has become an important production region in China. Coal mining in this region is often faced with hard roof conditions and extra-thick coal seams, of which the extra-thick hard roof is of good integrity and high strength. However, under this condition, the roof is difficult to collapse in time and the gob is suspended in a large area (Wang et al. 2015; Zhao et al. 2017). During coal mining, roadways are affected by the mining of adjacent working faces (Li et al. 2023; Mao et al. 2023). Especially, when the mining height is large and the roof is hard and easy to form a stress transmission structure, it is easy for dynamic phenomena to occur such as rockbursts when the rock stratum collapses. For roadways where extra-thick coal seams and extremely thick hard roof conditions coexist, the mining-induced stress is more intense and the influence range is wider (Gong et al. 2021). Traditional roof reinforcement materials are prone to fracture failure (Jiang et al. 2023; Li et al. 2016; Wang et al. 2021a), which can no longer meet the ground control requirements of such roadways. Aiming at solving the problems of dynamic pressure and rock deformation control in roadways, scholars have conducted extensive studies on pressure relief and support control.

In terms of roadway pressure relief, Gao et al. (2013) adopted the method of forced caving by blasting to reduce the additional stress of the filling side next to the roadway and to prevent the filling side of the hard roof of the deep shaft retained along the gob from being crushed when the roof collapses. Yang and Zheng (2020) studied the overburden displacement of the thick coal seam under fully mechanized caving mining, and proposed a hydraulic fracturing impact prevention method for hard roof, which can reduce the roof weighting step distance, dynamic load coefficient, and maximum pressure. Wang et al. (2021b) developed a method of high-strength anchor grouting, roof cutting, and self-formed roadway. This method uses high-strength bolt grouting to improve the integrity of the roadway roof, and uses the directional roof pre-splitting to cut off the stress transfer path between roofs. The experimental results show that the rock stress after this treatment is on average 20.8% lower than that of the gob side entry, and the rock deformation is 45.1% that of the latter. The studies described above show that pressure relief technologies such as forced caving by deep hole blasting, hydraulic fracturing, and roof pre-splitting and coal seam cutting can change the roof stress transfer path and reduce the stress above the roadway. The pressure relief technology of roof pre-splitting and coal seam cutting greatly reduces the stress concentration magnitude

and range, which can completely cut off the physical connection between the gob and the roadway roof along the strike direction of the roadway (He et al. 2015; Wang et al. 2020a, b).

In terms of roadway support, Kang et al. (2018) proposed to use high-strength, high-toughness bolts to safely control the surrounding rock of the roadway. Based on the excellent performance of NPR (negative Poisson's ratio) structure in impact resistance, energy absorption, and yield, He et al. (2014) developed a constant-resistance energy-absorbing anchor cable with NPR structure. The anchor cable allows for the large deformation of the support material under constant resistance conditions and has good energy absorption and impact resistance. Wang et al. (2022a) established a constant-resistance energy-absorbing bolt with high strength, high elongation, and high pre-tension, which has good impact resistance and overall deformation capacity. In short, the use of energy-absorbing reinforcement can effectively absorb the energy accumulated in the surrounding rock of the roadway (Wang et al. 2022b), improve the erosion resistance of the reinforcement system, and help control the rock deformation caused by the collapse of the thick hard roof.

In this work, we propose a ground control method using roof cutting for pressure releasing and energy-absorbing reinforcement for extra-thick hard roof roadway. Furthermore, we conduct numerical and physical models to compare the results, and discuss the advantages of roof cutting pressure relief and energy-absorbing reinforcement in roadway ground control. Finally, this method has been successfully applied to the field and monitored results suggest the effectiveness and rationality of the new method.

2 Ground Control for Roadway with Extra-Thick Hard Roof

2.1 Principles

The reasons for the difficulty in controlling the surrounding rock of roadway with extra-thick hard roof are: (1) The extra-thick hard roof above the working face is of high strength and is difficult to collapse, and the large suspended roof is prone to form stress concentration and energy accumulation in the rock. (2) Under the condition of extra-thick coal seam, the mining disturbance is severe, and the collapse of the large suspended roof has a greater impact on the dynamic pressure. (3) Under the influence of large dynamic stress, the traditional roadway reinforcing materials are prone to failure due to insufficient elongation and poor energy-absorption capacity, and the roadway faces the risk of dynamic disasters such as mine earthquakes.

To this end, we propose the integrated concept of roof cutting for pressure releasing and energy-absorption reinforcement: (1) Before the mining of the working face,

directional roof cutting is applied to cut off the stress transfer path between the roadway roof and the gob roof for stress release. (2) At the same time, blasting is applied onto the roadway roof to accelerate the collapse of the hard roof while strengthen roof cutting and pressure relief, and reducing the impact of the collapse on the roadway. (3) After the comprehensive pressure relief described above, the constant-resistance energy-absorbing reinforcement is implemented. The method allows the extra-thick and hard roof above the roadway to form an integrated structure, absorb the strain energy when the thick and hard roof in the gob collapses, so as to ensure the safety and stability of the roadway.

2.2 Control Method for Roadway with Extra-Thick Hard Roof

Based on the principles, the control method of roof cutting for pressure releasing and energy-absorption reinforcement in hard roof roadway is proposed, as shown in Fig. 1.

The technical principles of this method are:

1. The roof of the roadway near the gob side is directionally cut by using the characteristics of low-tension resistance of rocks. It makes roof blastholes create concentrated tension in presplitting direction. When multiple adjacent blastholes are simultaneously blasted, the directional crack generates and penetrates the surrounding rocks to form a directional roof presplitting surface. In this way, the stress transfer path of the roadway and the overlying roof of the gob can be cut off, so that the gob roof can collapse directionally along the cutting surface under the action of the mining-induced stress and the gravity of the rock stratum, as shown in Part I of Fig. 1.

2. After directional cutting, the gob roof is blasted to collapse. In addition to strengthen the roof cutting for pressure release, the blasting accelerates the collapse of the hard roof, thereby reducing the impact of large gob roof collapse on the roadway.

3. Constant-resistance energy-absorbing anchor cables are used to reinforce the roadway roof and absorb the strain energy of the rock in the event when the extra-thick roof collapses in the gob, as shown in Part II of Fig. 1. The combined energy-absorption reinforcement and pressure releasing measures constitute an integrated ground control system, which ensures the safety and stability of the surrounding rock of the roadway when the thick and hard roof collapses in the gob during mining.

2.3 New Type Constant-Resistance Energy-Absorbing Anchor Cable

The constant-resistance energy-absorbing anchor cable is the key reinforcing material for ground control, and its main body consists of a cable body and a constant resistance device, as shown in Fig. 2. When the stress of the anchor cable is lower than the designed constant resistance, the elastic deformation of the cable body will absorb the energy of the rock. When the stress of the anchor cable is greater than or equal to the designed constant resistance, the cable body slides along the inner side of the sleeve, and the anchor cable is deformed to absorb the rock energy (Wang et al. 2022b). The performance of the constant-resistance
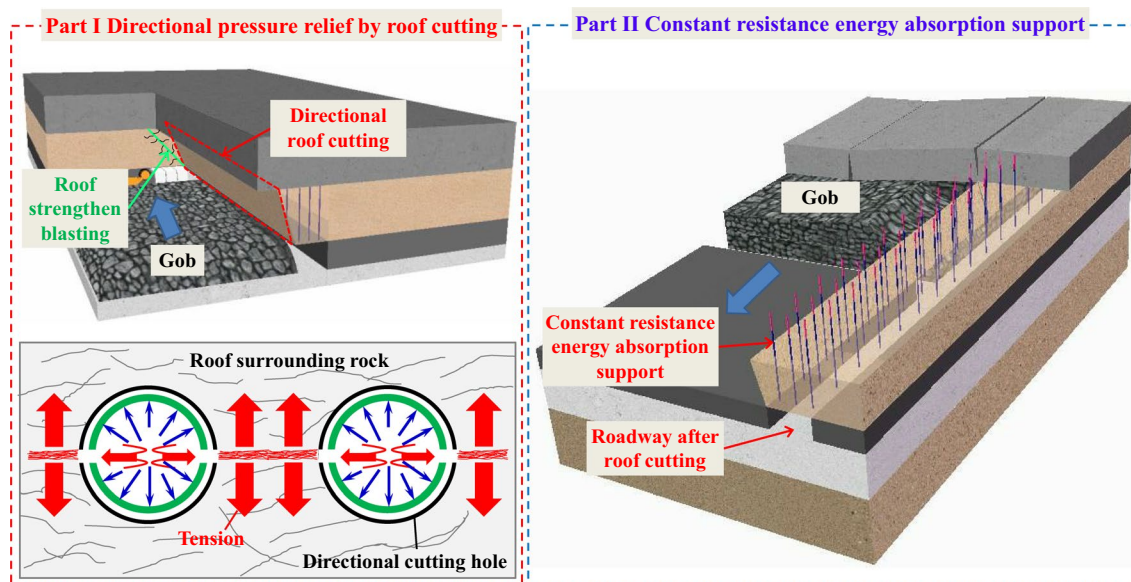

Fig. 1 Principles of roof cutting pressure releasing and energy-absorbing reinforcement
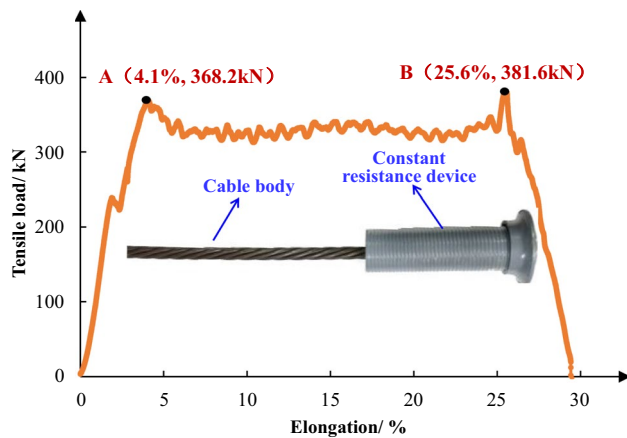
Fig. 2 Performance of the constant-resistance energy-absorbing anchor cable under tension

energy-absorbing anchor cable under tensile load is shown in Fig. 2.

1. The constant-resistance energy-absorbing anchor cable exhibits elastic stage and constant resistance stage. (a) Elastic stage (section $0 \rightarrow A$): load and elongation are approximately linear; (b) Constant resistance stage (section $A \rightarrow B$): after the load reaches 368.2kN (point A), the constant-resistance body slides along the inner side of the constant-resistance sleeve, and the constant load fluctuates in the range of 313.1–381.6 kN.
2. The maximum elongation of the anchor cable is 25.6%, and the energy absorbed per unit length is 12.7×10^4 J.

The maximum elongation of traditional anchor cables can reach about 3–7%, and the energy absorbed per unit length is 0.8×10^4–1.8×10^4 J (Li et al. 2023). The absorbed energy of the former is 7.1–15.9 times that of the latter. It can be seen that the constant-resistance energy-absorbing anchor cable has larger energy-absorption capacity while maintaining higher constant resistance.

3 Numerical Test of Roof Cutting for Pressure Release Control

3.1 Engineering Background

The Caojiatan Coal Mine is located in western China. The #122108 working face of the mine is buried 300–363 m, the length along the strike is 5,910 m, the length along the dip is 280 m, the average thickness is 10.60 m, the mining height is 5.8 m, and the caving height is 5–6 m. The roof above the working face in the ventilation roadway is mainly sandstone, which is 2.22 m thick fine sandstone, 4.20 m thick siltstone, and 21.20 m thick medium sandstone from the bottom to the top. The total thickness of sandstone is 27.62 m, which belongs to a typical extra-thick and hard roof. Among them, the medium sandstone is the key rock stratum, with a compressive strength of 52.1 MPa and a tensile strength of 7.8 MPa. In the mining stage of the working face, the mining-induced stress is high, the floor and sides are severely deformed, and the reinforcing system is failed in some locations, as shown in Fig. 3.

Fig. 3 Borehole histogram and layout of the working face
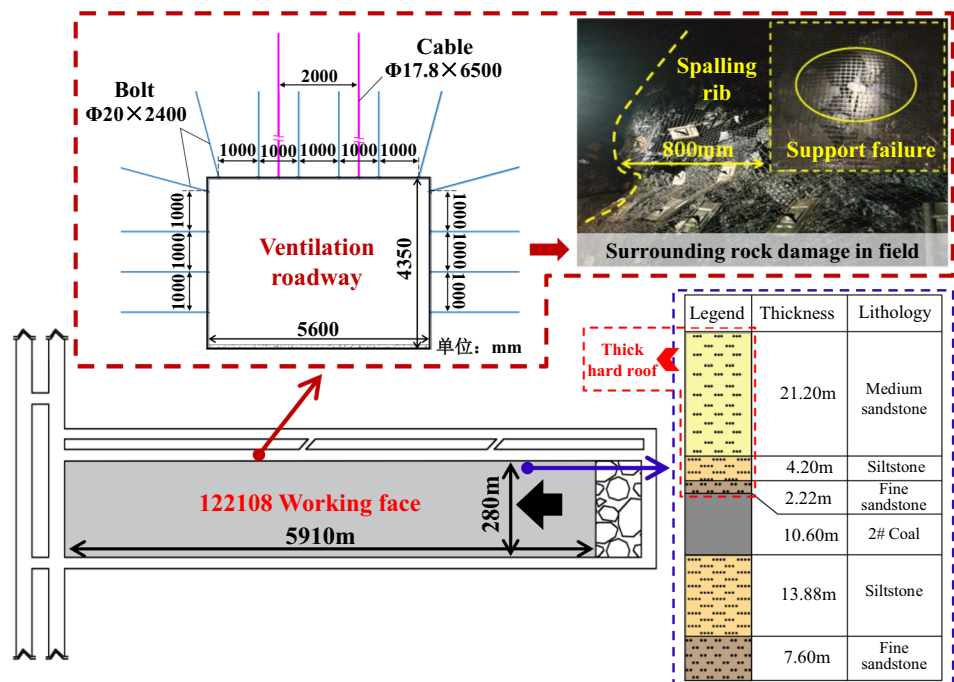
We take this working face as the engineering background to conduct numerical tests on directional roof cutting for pressure release and discuss the advantages of this method in the ground control of such roadways.

3.2 Conceptual Design

The selection of pressure relief parameters is crucial to the effect of ground control (Wang et al. 2022c; He et al. 2021, 2018). The designed parameters include roof cutting parameters and strengthen blasting parameters. Roof cutting parameters include Type A scheme (different roof cutting angles) and Type B scheme (different roof cutting heights). Strengthen blasting parameters are in Type C scheme (different blasting angles).

For Type A to C schemes, a FLAC^{3D} model with the same field dimension, geomechanical parameters, and reinforcing parameters is established. The roadway section size, rock reinforcing strength, and coal seam thickness of the Caojiatan Coal Mine are taken as constant, while the roof cutting angle, roof cutting height, and blasting angle are variables. The schemes are described as follows.

Type A scheme (different roof cutting angles): Roof cutting angles, (Ai, $i = 1$–5), are 0°, 10°, 20°, 30° and 40°. According to the field condition, the roof cutting height in this scheme is 30 m, and the details are provided in Table 1.

Type B scheme (different roof cutting heights): Top cutting height, (Bi, $i = 1$–5), are 5 m, 10 m, 20 m, 30 m and 40 m. The roof cutting angle is constant, which is taken according to the optimal roof cutting angle in Type A scheme, and the details for this scheme are listed in Table 2.

Type C scheme (different blasting angles): the blasting angle is used as a variable to study the promotion effect of strengthen blasting on the roof cutting pressure relief. The blasting angle in this section is defined as the deviation from the roof cutting direction. The blasting angle scheme is represented by Ci, $i = 1$–5, and the corresponding blasting angles are 0°, 5°, 10°, 15° and 20°, respectively. In Type C scheme, the cutting angle and height are selected according to the optimal parameters determined after the comparative analysis of Type A and Type B schemes. And the blasting height is selected according to the roof cutting height of the best ground control in Type B scheme. The specific details are provided in Table 3. The physical and mechanical parameters of the rock mass are shown in Table 4. In simulating the weaking effect due to blasting, the mechanical parameters of the rock mass in the fragmentation area are reduced to 1/5 of the original values (Xiong and He 2006; Zhu et al. 2021).

3.3 Establishment of Model and Evaluation Index

3.3.1 Model Establishment

According to the field geological conditions, we build a numerical model with a dimension of $330 \times 144 \times 180$ m (width × length × thickness). The Mohr Coulomb criterion is used as the constitutive model. The bottom boundary of the model is fixed in the vertical direction, the front, back, left, and right boundaries are fixed in the horizontal direction, and the upper boundary is applied with the overburden stress. The monitoring section is set at 90 m from the front boundary of the model, and the monitoring points are set at the roadway roof, floor, and solid coal rib

Table 1 Type A scheme for different cutting angles

Test no.	Roof cutting angle/°	Constant
A1	0	Roof cutting height
A2	10	No strengthen blasting
A3	20	
A4	30	
A5	40	

Table 2 Type B scheme for different cutting heights

Test no.	Roof cutting height/m	Constant
B1	5	Roof cutting angle
B2	10	No strengthen blasting
B3	20	
B4	30	
B5	40	

Table 3 Type C scheme for different blasting angles

Test no.	Blasting angle/°	Constant
C1	0	Roof cutting height
C2	5	Roof cutting angle
C3	10	Blasting height
C4	15	
C5	20	

Table 4 Physical and mechanical parameters of the rock mass

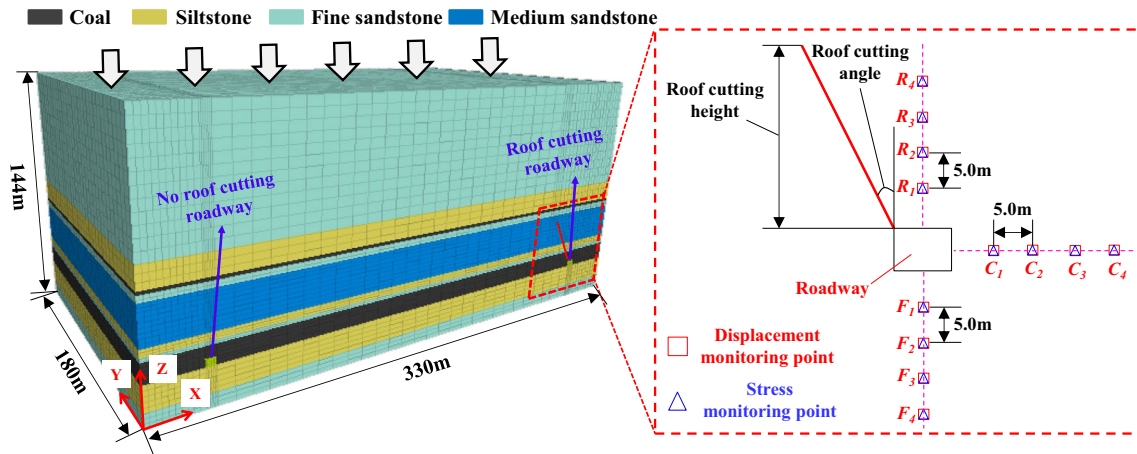| Lithology	Bulk modulus/ GPa	Shear modulus/ GPa	Tensile strength/ MPa	Internal friction angle/°
Medium sandstone	14.0	4.2	1.6	41.3
Siltstone	24.8	10.4	2.1	49.3
Fine sandstone	15.0	4.8	2.4	40.9
Coal	9.6	4.0	0.4	39.7

Fig. 4 Schematic diagram of the model and monitoring scheme

side, represented by R_w, F_w, and C_w, respectively, w = 1–4. The interval between the measurement points is 5 m, as shown in Fig. 4.

3.3.2 Establishment of Evaluation Index

By calculating the mean stress of the monitoring points at the same distance from the roadway boundary, we analyze the rock within 5–20 m of the roadway roof, floor, and rib side. For example, the average rock stress at 5 m from the roadway boundary is $\overline{S_1} = (R_1 + C_1 + F_1)/3$, and the average rock stress at 10 m from the roadway boundary is $\overline{S_2}$.

Next, the evolution of rock stress in different schemes will be compared and analyzed to examine the effect of pressure relief. The quantitative evaluation index $\delta_{R_{ij}}$ of stress reduction rate is established to analyze the effect of pressure relief and control, which is defined as the percentage of the average stress reduction of the rock with roof cutting versus that without roof cutting,

$$\delta_{R_{ij}} = (\overline{R}_0 - \overline{R}_{ij})/\overline{R}_0 \times 100\%, \tag{1}$$

where $\delta_{R_{ij}}$—Average stress reduction rate of the rock in scheme ij. The higher the $\delta_{R_{ij}}$, the more significant the impact of roof cutting. i represents the number of different types of schemes, $i = A$–C, j represents the sub-schemes under the general scheme, and $j = 1$–5. For example, $\delta_{R_{A1}}$ represents the average stress reduction rate of the rock in A1 scheme, %.

$\overline{R}_0$—Average stress of the rock without roof cutting, MPa.
$\overline{R}_{ij}$—Average stress of the rock in ij scheme, MPa.

Based on the stress reduction rate of the rock, the types of schemes are compared and analyzed, and the sub-scheme with the largest stress reduction rate in each scheme is taken as the optimal scheme. In addition, the stress reduction rate

of the optimal scheme is taken as the benchmark and its first integer value as the limited range, which is used as the reference interval for comparing the pressure relief effect of each sub-scheme. For example, if the maximum stress reduction rate δ_R in each scheme is 24%, then $20\% < \delta_R < 24\%$ is the reference range for the comparison and selection of the pressure relief effect of each sub-scheme, and all sub-schemes with stress reduction rate within this range can be regarded as reasonable schemes.

3.4 Result Analysis

#### 3.4.1 Analysis of Different Pressure Relief Parameters

1. Analysis of different top cutting angles
   Figure 5 shows the stress distribution and evaluation index of the roadway rock under different roof cutting angles (A1–A5 schemes).
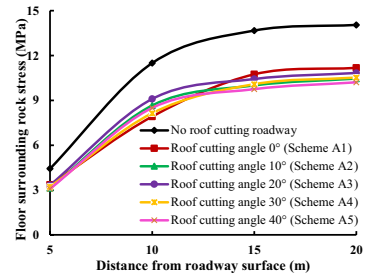
   1. In the different cutting angle schemes (A1–A5 schemes) of the roadway, the rock stress shows a trend of increasing first and then stabilizing as a function of distance away from the roadway surface, while the stress of the solid coal rib side shows a trend of decreasing first and then stabilizing. Affected by directional roof cutting, the average rock stress within 5–20 m from the roadway surface is generally lower than that of the rock without roof cutting, as shown in Fig. 5a–c.

   2. The maximum average rock stress of the roadway without roof cutting appears at 10 m from the roadway surface, while the maximum average stress of the roadway with roof cutting appears at 15 m or even 20 m from the roadway surface. The rock stress with roof cutting is significantly lower than of the rock without cutting, as shown in Fig. 5d.
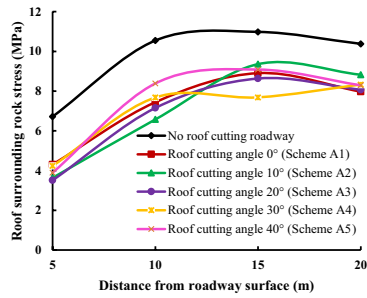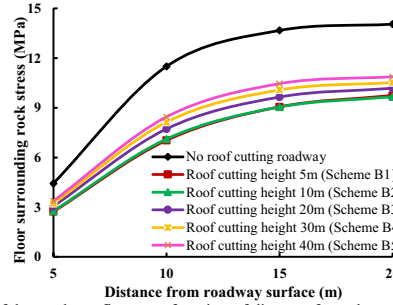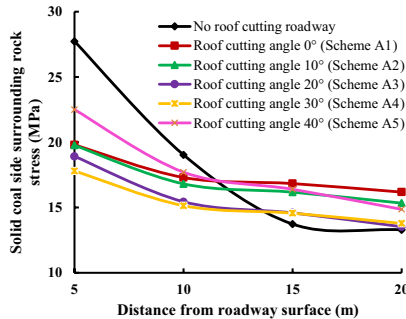
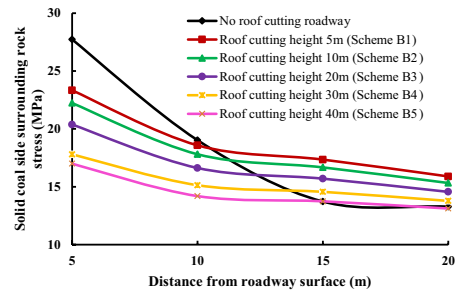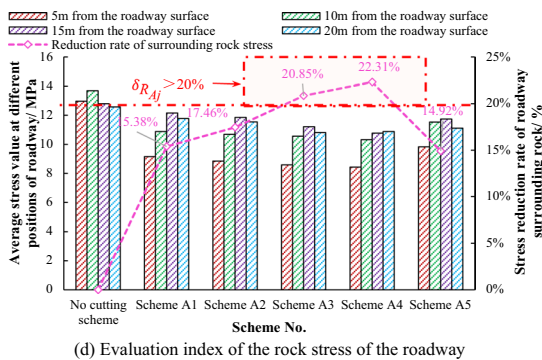(a) Stress of the roadway roof as a function of distance from the roadway surface
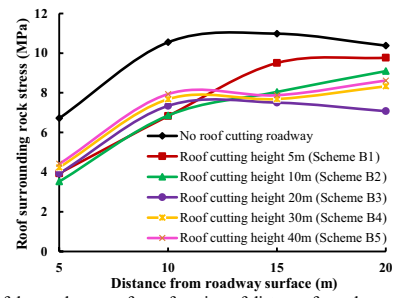
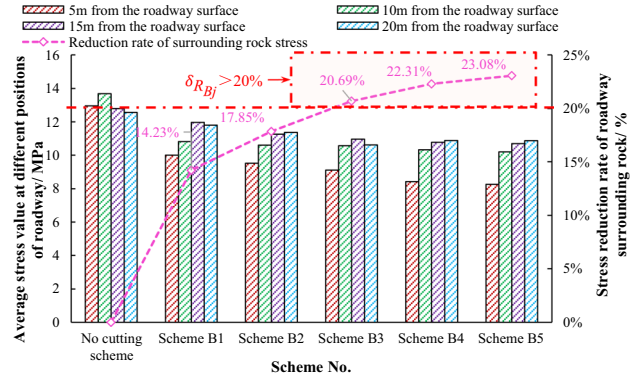(b) Stress of the roadway floor as a function of distance from the roadway surface

(c) Stress of the solid coal rib side as a function of distance from the roadway surface

(d) Evaluation index of the rock stress of the roadway

Fig. 5 Stress evolution and evaluation index of roadway with different roof cutting angles

(a) Stress of the roadway roof as a function of distance from the roadway surface

(b) Stress of the roadway floor as a function of distance from the roadway surface

(c) Stress of the solid coal rib side as a function of distance from the roadway surface

(d) Evaluation index of the rock stress of the roadway

Fig. 6 Stress evolution and evaluation index of the roadway with different roof cutting heights

3. With the increase of the roof cutting angle, the stress reduction rate increases first and then decreases. In the 30° roof cutting scheme (A4), the stress reduction rate of the rock reaches the maximum of 22.31%. Therefore, this roof cutting angle has the best effect on the stress release, as shown in Fig. 5d. The stress reduction rate in A3 scheme and A4 scheme is in the range of $20\% < \delta_R < 22.31\%$. There-

fore, the reasonable range of the roof cutting angle is 20°–30°.

In short, when the roof cutting angle is 30°, the optimal cutting control effect can be obtained for the roadway under this condition. Therefore, according to these optimized parameters, B type is used in the numerical

comparison test to further study the control effect of different roof cutting heights on the roadway.

2. Analysis of different roof cutting height schemes

   Figure 6 shows the stress distribution and evaluation index of the roadway in different roof cutting height schemes (B1–B5 schemes).

   1. The stress of the roadway in each roof cutting scheme is smaller than that of the roadway without roof cutting. With the increase of the cutting height, the stress of the roadway roof and solid coal rib side decreases, and the stress of the roadway floor increases, as shown in Fig. 6a–c. The increase of the cutting height increases the range and weight of the cantilever beam of the roadway roof, which may lead to an increase in the stress of the roadway floor.

   2. The maximum stress of the rock with roof cutting occurs at a distance 15 m or even 20 m away from the roadway surface. The stress of the rock with roof cutting is significantly lower than that of the rock without cutting, which is similar to the effect of the roof cutting angle.

   With the increase of cutting height, the stress reduction rate of the rock first increases rapidly and then slowly increases. In the 40 m cutting height scheme (B5), the rock stress reduction rate reaches the maximum of 23.08%. Therefore, 40 m is the cutting height that can achieve the best stress release effect. The schemes with reduction rate in the range of $20\% < \delta_R < 23.08\%$ are the B3–B5 scheme. In this range, as the roof cutting height increases, the increment of stress reduction rate gradually decreases. Considering field conditions, the cutting height of the roof r should not be too large (more than 30 m), and the reasonable cutting height is 20–30 m.

   According to the above optimized parameters, the C type numerical comparison test was used to study the facilitation effect of different strengthen blasting angles on the pressure relief of the roadway. The strengthen blasting height is constant, and it is set the same as the optimal cutting height.

3. Analysis of schemes with different blasting angles

   Figure 7 shows the stress distribution and evaluation index of roadway rock in different blasting angle schemes (C1–C5 schemes).

   1. In the scheme of different strengthen blasting angles (C1–C5 schemes). With the increase of the blasting angle (from 5° to 20°), the stress of the roadway floor decreases first and then remains basically unchanged, while the stresses of the roof and the rib side do not change much, as shown in Fig. 7a–c. The results show that the change of blasting angle has a greater influence on the roadway floor than other segments of the roadway.
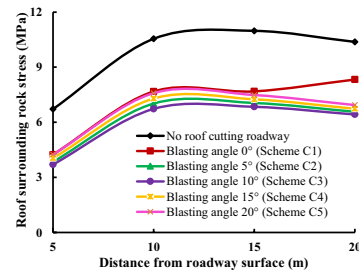
   2. With the increase of the blasting angle, the rate of rock stress reduction first increases and then decreases. The stress reduction rate reaches the maximum of 34.15% at the blasting angle of 10° (C3 scheme). Therefore, the 10° blasting angle has the

(a) Stress of the roadway roof as a function of distance from the roadway surface

(b) Stress of the roadway floor as a function of distance from the roadway surface
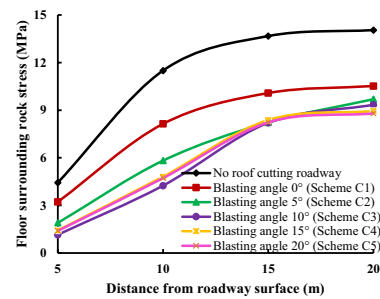
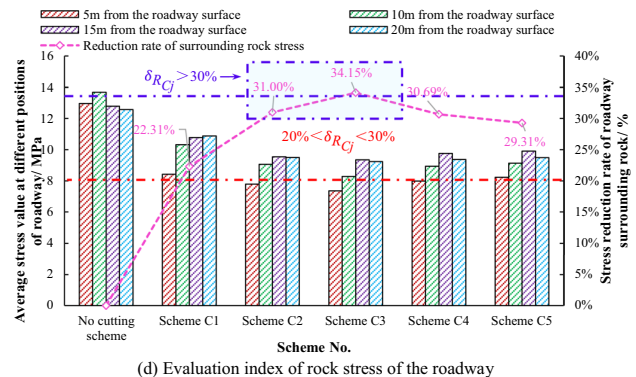(c) Stress of the solid coal rib side as a function of distance from the roadway surface
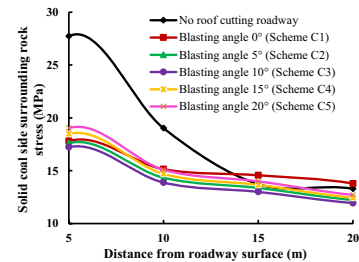
(d) Evaluation index of rock stress of the roadway

Fig. 7 Stress evolution and evaluation index of the roadway in different roof blasting angles

best auxiliary pressure relief effect on the rock stress of the roof-cutting roadway, as shown in Fig. 7d. The schemes within the range of stress reduction rate of $30\% < \delta_R < 34.15\%$ are C2–C4 schemes, therefore, the reasonable range of strengthen blasting angle is 5°–15°.

According to the above parameter analysis, it can be concluded that: in view of the extra-thick and hard roof roadway, the roof cutting height of 20–30 m and the cutting angle of 20–30° are the optimal range with significant pressure relief effect. Moreover, the strengthen blasting angle of 5°–15° away from the cutting direction is the optimal range, which enhances the release effect significantly.

3.4.2 Analysis of Stress Evolution

The directional roof cutting and strengthen blasting parameters of the roadway are designed according to the

reasonable selection range of the above parameters and in combination with the thickness of the roof. Specifically, the cutting height (vertical height) of the roof stratum is 28 m, the height (vertical height) of the strengthen blasting is 25 m, the angle of directional roof cutting is 30°, and the angle of the strengthen blasting is 10° different from the angle of the directional roof cutting.

The monitoring section is set in the middle of the strike length of the working face, as shown in Fig. 8a. The three-dimensional stress evolution of the surrounding rock is shown in Fig. 8b. X-axis represents the length of the working face in the direction of inclination, (m); Y-axis represents the distance between the monitoring section and the excavation position of the working face, (m), and "-" indicates that the monitoring section is located before the excavation position of the working face; and Z-axis represents the vertical stress in the surrounding rock, (MPa).

1. The mining-induced stress at roadway position with original reinforcement without roof cutting on the left
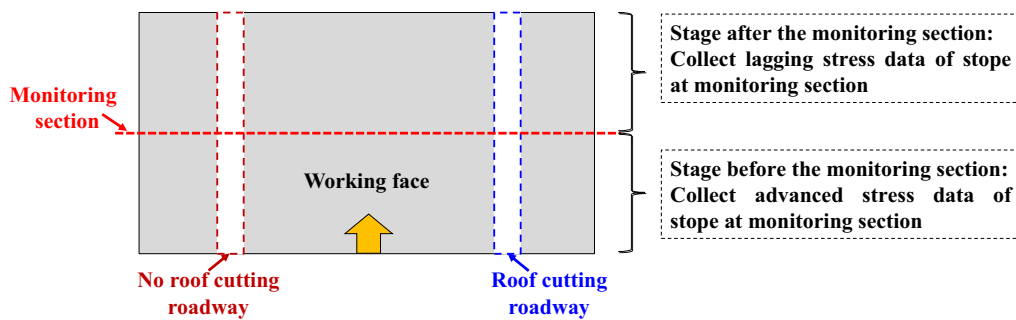
(a) Schematic diagram of three-dimensional stress monitoring of the rock
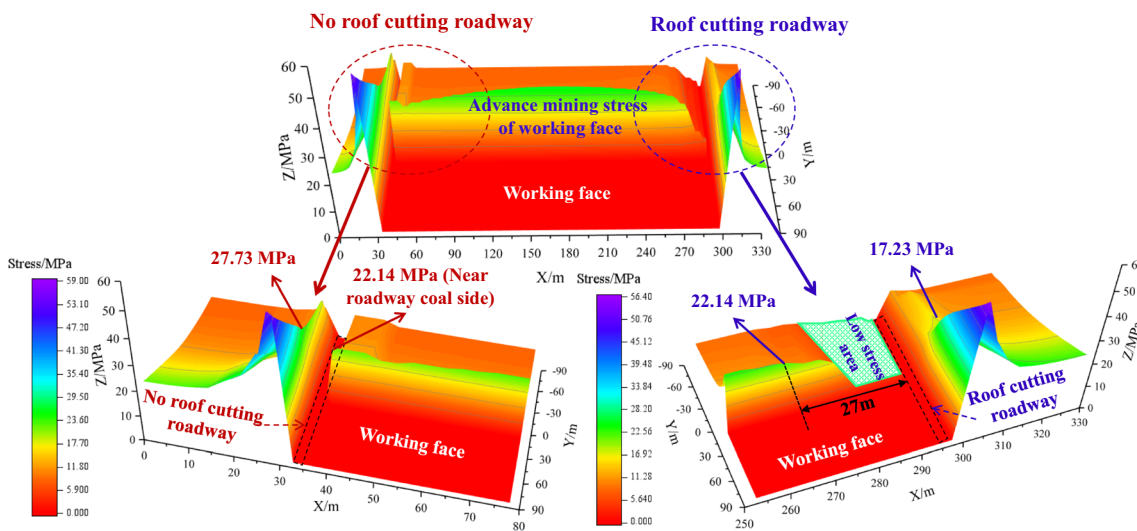
(b) Three-dimensional stress contour of the rock

Fig. 8 Three-dimensional stress evolution of the roadway

side of the working face is 22.14 MPa, which is close to that of the coal rib side of the roadway. However, the mining-induced stress at the working face at the right roof-cutting roadway is small, and a large range of low-stress area appears on the coal rib side. The pressure of the same magnitude as that of the left roadway occurs about 27 m away from the coal rib side of the right roadway. This shows that under the combined action of roof cutting pressure release and strengthen blasting, the right roadway exhibits obvious pressure relief effect.

2. Comparing the mining-induced stresses of the roof without cutting on the left side and of the roof with cutting on the right side of the working face, it can be seen that when the working face is behind the monitoring section (Y: 0–90 m), the size and evolution of the lateral bearing pressure of the solid coal rib side in the two types of roadways are similar. However, when the working face is ahead of the monitoring section (Y: − 90 to 0 m), there are large differences between the lateral bearing pressure of the solid coal rib side of the two roadways and the mining-induced stress at the coal side of the working face.

3. The maximum mining-induced stress of the solid coal rib side is 17.23 MPa on the right side of the working face with roof cutting, while it is 27.73 MPa on the left side of the working face without roof cutting. The former is 37.87% lower than the latter, indicating that under the combined action of roof cutting and strengthen blasting, the pressure relief effect on the solid coal rib side in the roadway is significant.

4 Physical Model Test

To verify the rationality and effectiveness of the numerical results in the previous section, we conduct corresponding physical model tests to examine roof cutting pressure relief and energy-absorption reinforcement for roadway with extra-thick hard roof. Subsequently, we compare the stress changes between numerical and physical models.

4.1 Experimental Apparatus

The three-dimensional physical model apparatus developed by the authors' group is used to carry out the model tests. The system consists of a hydraulic reaction loading system, a high-precision real-time monitoring system, an automatic coal mining and roadway driving system, and a directional roof cutting simulation system, as shown in Fig. 9. The automatic coal mining and roadway driving system includes coal mining simulation device, roadway driving simulation device and power stretching device. The first two devices are used for coal mining simulation and roadway driving
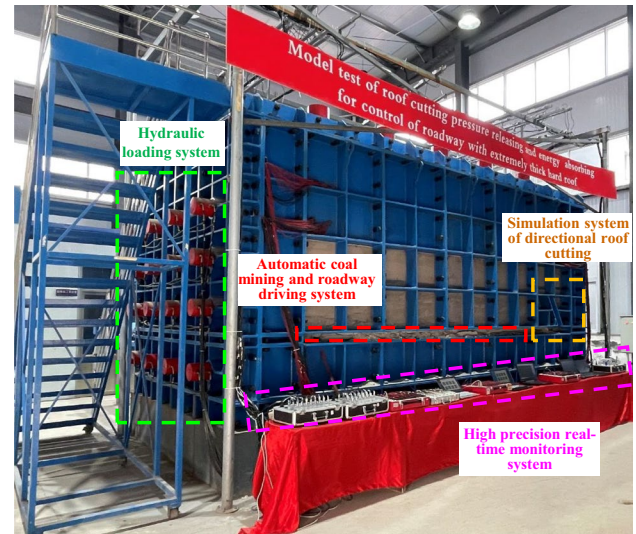

Fig. 9 Physical model test system

simulation, and the power stretching device is designed to accurately control them.

4.2 Experimental Design

4.2.1 Determination of Similarity Scale

The geometric similarity scale is $C_L = 60$, the unit weight similarity scale is $C_\gamma = 1.2$, and the stress similarity scale is $C_f = C_L \times C_\gamma = 72$. The field geological range of 330 m × 144 m × 180 m is selected for simulation, and the converted model size is 5500 mm × 2400 mm × 3000 mm.

The dimension of the model roadway is 93 mm × 72.5 mm (width × height), which is used to simulate the actual roadway size of 5.6 m × 4.35 m (width × height). According to the numerical results and the thickness of the actual roof stratum, the designed directional roof cutting height (vertical height) in the physical model is 467 mm, which corresponds to the actual height of 28 m. The designed strengthen blasting height (vertical height) in the model is 417 mm, corresponding to the actual height of 25 m. The directional roof cutting angle is 30°, and the strengthen blasting angle deviates from the directional roof cutting angle by 10°.

4.2.2 Test Schemes

The test sections of the roadways on both sides of the working face are selected for comparative analysis. The two test sections are represented by M1 and M2. Traditional reinforcement design was used in the test section M1 on the left side (actual field design), and pressure relief and energy-absorbing reinforcement was implemented in the test section
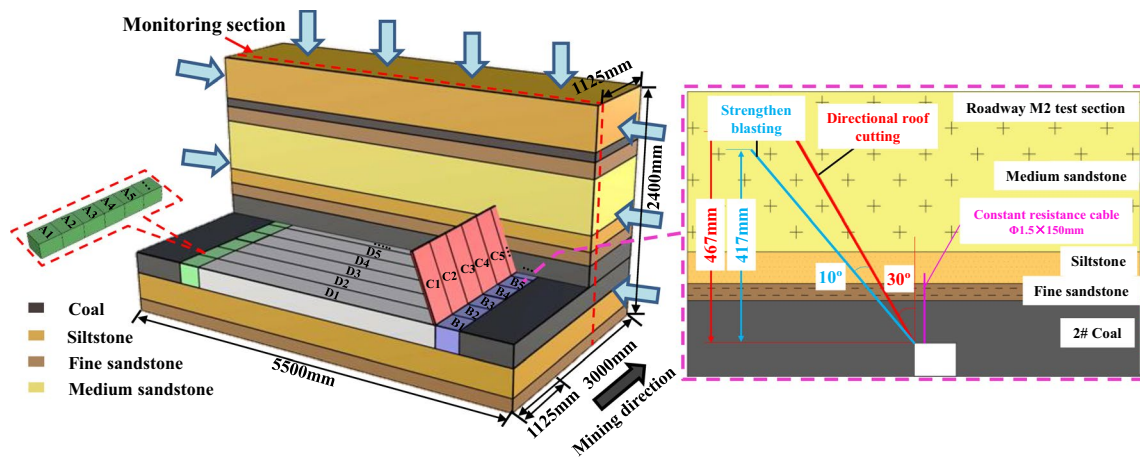
Fig. 10 Schematic diagram of the test schemes

Table 5 Scheme design of the physical model test

Test section number	Roadways	Pressure relief design	Reinforcement design
M_1	Left roadway	No pressure relief	Original support
M_2	Right roadway	Directional roof cutting + strengthen blasting	Energy-absorbing anchor cables

M2 on the right side. The test schemes are shown in Fig. 10 and Table 5.

1. Loading and excavation scheme

   Through the hydraulic reaction loading system, the vertical stress of the physical model is loaded to 0.114 MPa and the horizontal stress is loaded to 0.057 MPa. After the loading is completed, the excavation of the model body starts. The excavation sequence includes the following four stages: left roadway excavation Ai ($i = 1$–60, 60 steps, 50 mm each step) → right roadway excavation Bi ($i = 1$–60, 60 steps, 50 mm each step) → directional presplitting roof cutting Ci ($i = 1$–12, the directional roof cutting system works 12 steps ahead of the working face, 50 mm each step, 600 mm in total) → excavating the working face Di, ($i = 1$–60, 60 steps, 50 mm each step). The directional roof cutting is completed when the directional roof cutting system is fully drawn out. The strengthen blasting is realized by pre-buried mica sheets in the roadway roof according to the designed height and angle.

2. Monitoring scheme

   In the interior of the model body, a monitoring section 325 mm away from the front surface is placed along the strike direction of the simulated working face, which is used to monitor the stress and deformation of the traditionally reinforced section (M_1 section) and the roof cutting pressure relief energy-absorbing reinforced sec-

tion (M_2 section). The monitoring points, represented by R_i and F_j respectively, are arranged in the roadway roof and floor coal bodies. The positions of these monitoring points correspond to those of the monitoring points converted by geometric similarity scale in the previous numerical test.

4.3 Test Process

The model body is loaded according to the designed stresses. After the loading is stable, the model body is excavated, as shown in Fig. 11.

1. Roadway excavation stage on the left side of the working face: after the model is loaded, the roadway forming device embedded on the left side of the model is pulled at a constant speed, as shown in Step I of Fig. 11. The entire excavation process is divided into 60 steps, and excavation continues after each step is completed.

2. Roadway excavation stage on the right side of the working face: after the left roadway is excavated and stabilized, the right roadway forming device is pulled at a constant speed, as shown in Step II of Fig. 11. The excavation process is consistent with that of the left roadway.

3. Roof cutting stage of the right roadway: after the right roadway is excavated and stabilized, the directional roof cutting system of the right roadway is pulled at a constant speed to simulate the roof cutting and pressure
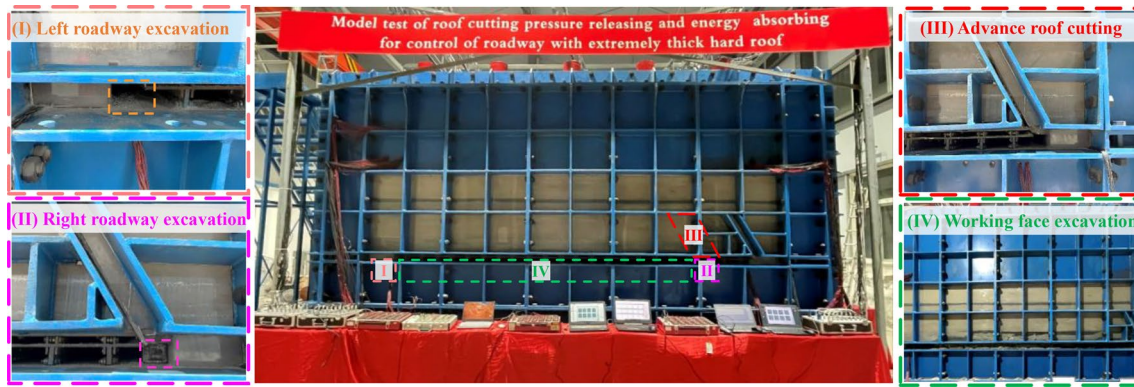
Fig. 11 Diagram of the test process

relief of the roadway, as shown in Step III of Fig. 11. The process is divided into 12 steps within 600 mm ahead of the right roadway, with each step pulling 50 mm.

4. Working face excavation stage: after the right roadway is 600 mm ahead of the directional roof cutting location and stabilized for a period of time, the mining sliding device of the working face and the directional roof cutting device of the right roadway are pulled at a constant speed. At the same time of mining the working face, the right roadway is subject to advanced directional roof cutting synchronously, as shown in Step IV of Fig. 11.

4.4 Analysis of Test Results

4.4.1 Data Validation

In this section, the roadway without roof cutting is compared with the roadway with roof cutting, and the stress change of the roadway at 4.5 m ahead of the working face is analyzed. The comparison of stress distribution in roadway roof and floor in the two types of tests is obtained, as shown in Figs. 12 and 13.

1. In the numerical simulation and physical model test, the stress evolutions in roadway roof and floor without and with roof cutting are similar. The stresses of the roadway roof and floor with roof cutting are lower than those of the roadway without roof cutting, indicating that the directional roof cutting pressure relief has advantages in the pressure relief of the roadway.

2. After stress conversion using similarity scale, the stresses of roadway roof and floor in the physical model are consistent with the field stresses in the numerical simulation. And the average stress difference is 11.44–26.87%.
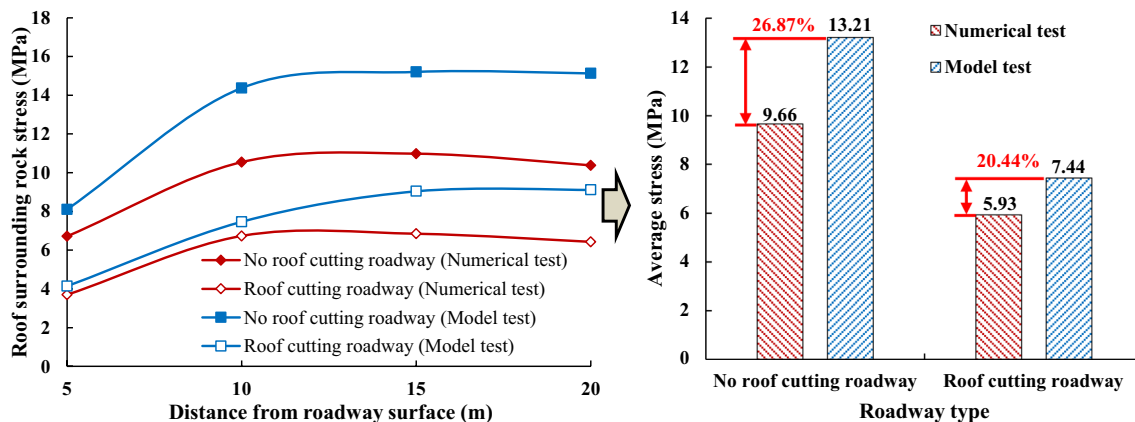

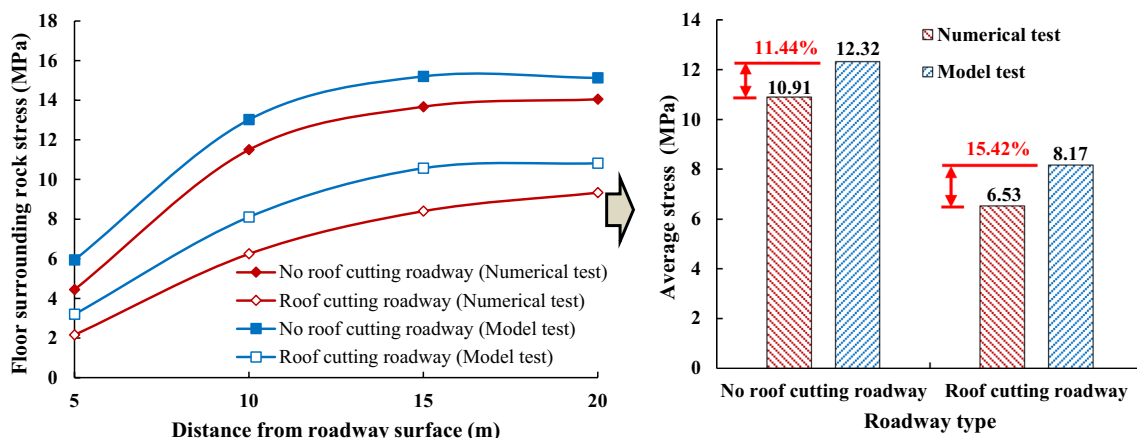**Fig. 12** Comparison of stress distribution in roadway roof

Fig. 13 Comparison of stress distribution in roadway floor

4.4.2 Comparison of Stress Evolution

Data of roadway roof monitoring points (R_1–R_2) and floor monitoring points (F_1–F_2) in the monitoring section are recorded. Stresses of roof and floor before the working face reaches the monitoring section (advanced working face, the distance is 0 to − 325 mm) and after the working face passes the monitoring section (lagging working face, the distance is 0–325 mm) along the mining direction are analyzed. Figures 14 and 15 show the stress evolutions of roadway roof and floor without roof cutting and under traditional reinforcement and with roof cutting with strengthen blasting and energy-absorbing reinforcement are obtained.

1. For the roadway after directional roof cutting, the stress at the shallow monitoring point (R_1) of the roof is always low, with the maximum not exceeding 0.068 MPa, which

is 40.87% lower than the maximum stress (0.115 MPa) at the shallow monitoring point of the roof of the roadway without roof cutting. The shallow monitoring point of the floor (F_1 5 m from the roadway floor surface) is in a low stress state during the advanced and the lagging working face stages relative to the monitoring section, which is mostly not affected by the mining of the working face.

2. The stresses of the roof and floor of the roadway with directional roof cutting are lower than that of the roadway without roof cutting. Further, the stress rapidly reduces to a low stress state after the working face passes the monitoring section. However, the stresses of the roof and floor of the roadway without roof cutting are in a large stress state in the stage when the monitoring section is ahead of the working face. And the stress
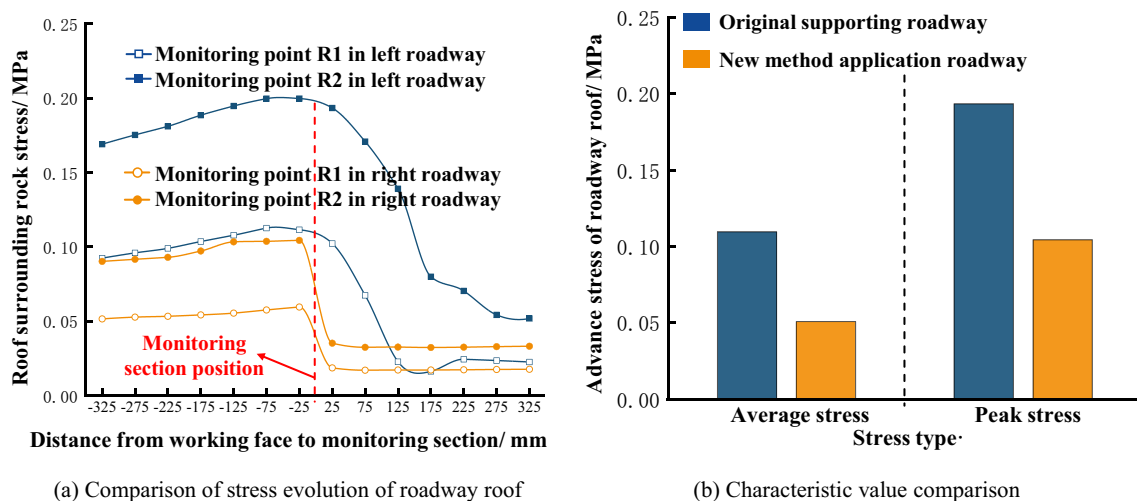

(a) Comparison of stress evolution of roadway roof

(b) Characteristic value comparison

Fig. 14 Stress variation of roadway roof

(a) Comparison of stress evolution of roadway floor

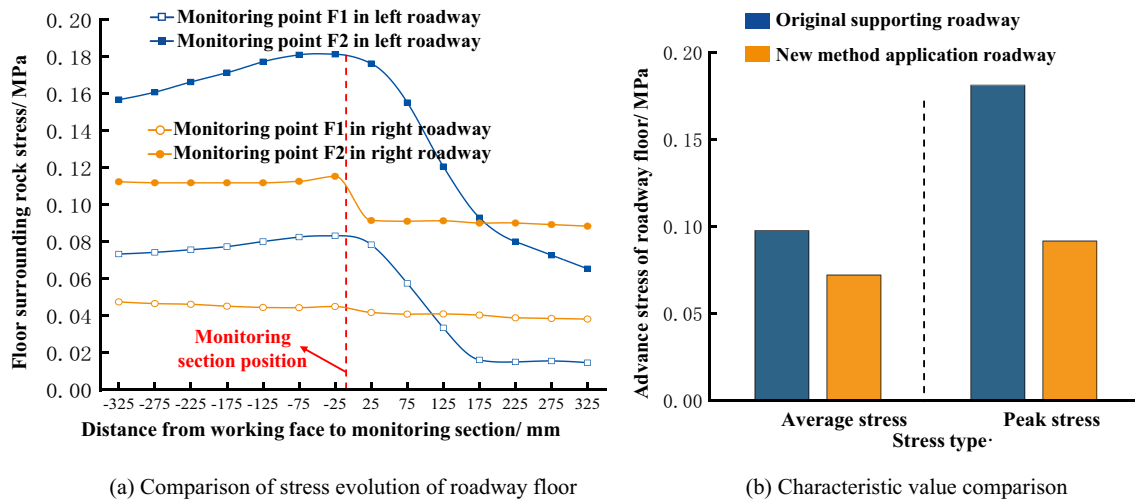(b) Characteristic value comparison

Fig. 15 Stress variation of roadway floor

starts to slowly reduce in the stage when the monitoring section is behind the working face.

3. In the roadway treated by directional roof cutting combined with strengthen blasting and energy-absorbing reinforcement, the stress of the roof and floor is reduced to a certain degree. The average stresses of the roof and floor of the roadway with roof cutting are 53.74% and 26.26% lower than that of the roadway without roof cutting, and the peak stresses are 46.02% and 49.61% lower, respectively. This indicates that directional roof cutting has a good pressure relief effect on surrounding rock of the roadway roof and floor.

4.4.3 Comparison of Deformation Evolution

We analyze the displacement data of R_1 monitoring point of the roadway roof and F_1 monitoring point of the floor in the monitoring section, as shown in Fig. 16.

1. The rock deformation of the roadway floor in the advanced working face is generally greater than that of the roadway roof, which suggests that the roadway floor is more affected by the mining-induced stress during mining the working face due to the influence of the extra-thick hard roof, and the deformation of the floor without reinforcement is significantly larger.
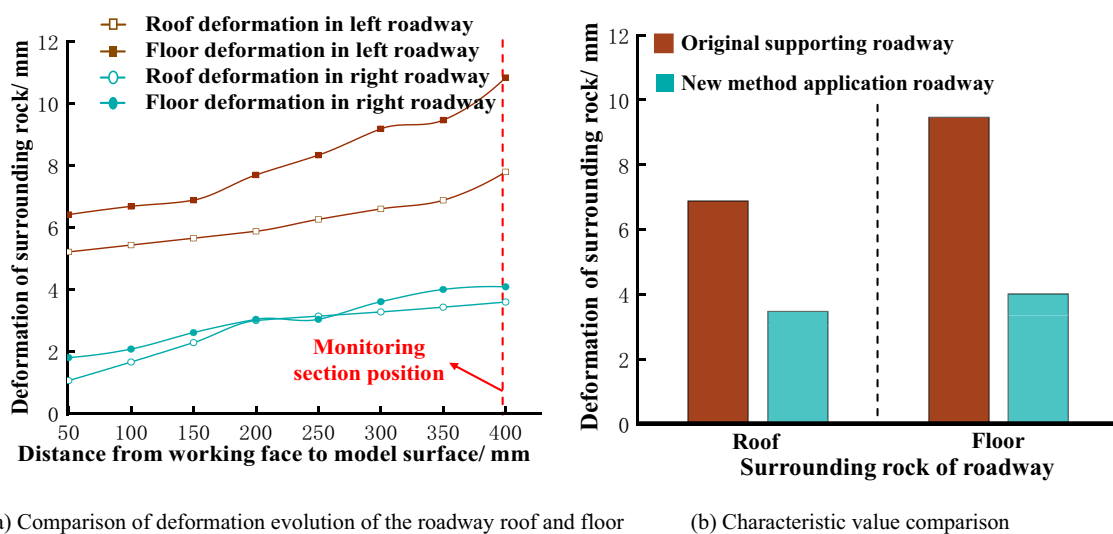

(a) Comparison of deformation evolution of the roadway roof and floor

(b) Characteristic value comparison

**Fig. 16** Deformation evolution of the roadway roof and floor

2. Compared with the traditionally reinforced roadway without roof cutting, the rock deformation of the roadway with directional roof cutting combined with strengthen blasting and energy-absorbing reinforcement is lower than that of roadway without roof cutting. The maximum roof deformation of the advanced working face is 3.43 mm, and the floor deformation is 4.01 mm. The maximum roof and floor displacements of the roadway are decreased by 54.47%, which implies that the method of directional roof cutting combined with strengthen blasting and energy-absorbing reinforcement has good reinforcing effect on the deformation of the roadway roof and floor.

### 4.4.4 Characteristics of Overburden Collapse at the Working Face

With the mining of the working face, the roof strata of the roadways on both sides have collapsed to varying degrees.

The characteristics of the overburden collapse at the working face are shown in Fig. 17.

1. Roadway without roof cutting on the left side of the working face: when the working face is mined for a certain distance, the hard roof near the gob on the left side of the roadway form a suspended roof within a certain range, as shown in the left schematic of Fig. 17a. When the area of the suspended roof reaches a certain extent, with the continuous mining of the working face, the suspended roof suddenly breaks, rotates, and sinks. One end is connected with the roadway roof, and the other end is connected with the collapsed roof of the gob, as shown in the right schematic of Fig. 17a.

2. Roadway with directional roof cutting on the right side of the working face: when the working face is mined for a short distance, the hard roof near the gob on the right side of the roadway will collapse along the directional cutting seam, as shown in the left schematic of Fig. 17b. With the continuous mining of the working face, the
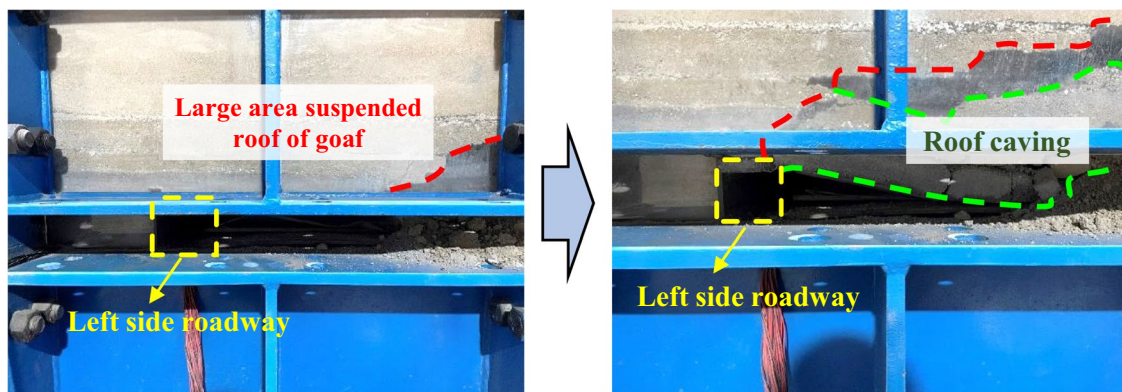
(a) Roadway with roof cutting on the left side of the working face
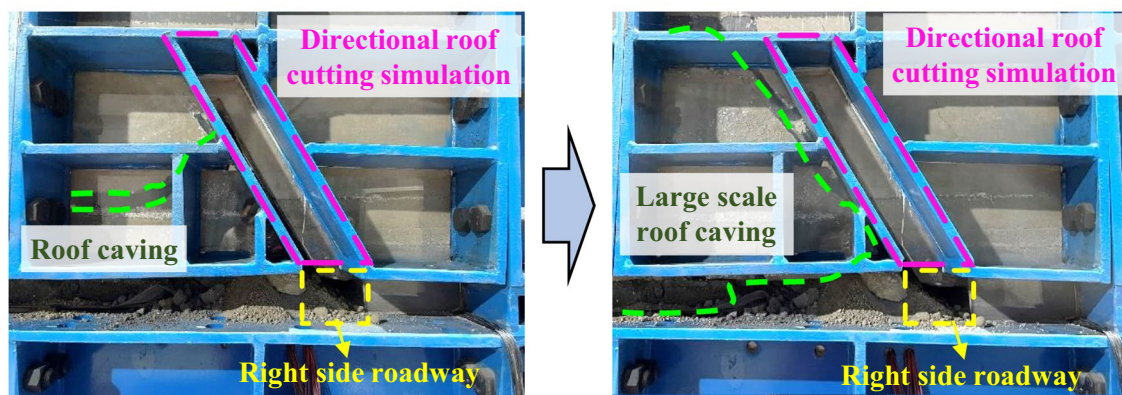
(b) Roadway with directional roof cutting on the right side of the working face

Fig. 17 Comparison of roof collapses of roadways and working faces

hard roof in the gob near the roadway continues to collapse to varying degrees. However, the surrounding rock of the roadway is basically not affected by the collapse of the roof of the whole working face, as shown in the right schematic of Fig. 17b.

3. Comparison of roadways on both sides: the mining distance when the roof of the working face on the right side collapses for the first time is far less than that of the roadway without roof cutting on the left side. This indicates that the physical connection between the roadway roof with directional roof cutting and the roof of the working face is cut off. Under the action of deep hole directional roof cutting, the roof of the gob can collapse rapidly, which solves the issue of large roof suspension in the gob of the hard roof roadway. The sudden collapse of a large suspended roof near the left roadway without roof cutting has a great impact on the roadway, and the large stress in the gob is transmitted to the roadway through the roof stress transmission structure.

5 Field Application

5.1 Roof Cutting Parameters and Reinforcement Design

Combined with the results of numerical simulation and physical model test, the parameters of directional roof cutting and energy-absorbing reinforcement were designed and applied in the ventilation roadway of the Caojiatan #122108 working face. The directional cutting height is 28 m, and the cutting angle is 30°, the strengthen blasting height is 25 m, and the strengthen blasting angle is 10°. The constant-resistance energy-absorbing anchor cable is located on the side of the roof cutting, its model is $\Phi22 \times 9000$ mm and its row spacing is 2000 mm. Specific directional pressure relief parameters and field reinforcement design are shown in Fig. 18.

5.2 Analysis of Monitoring Results

5.2.1 Monitoring and Analysis of Roadway Rock Deformation

With the new method applied, six deformation monitoring stations are arranged within 0–100 m of the test section, with an interval of 20 m. Two monitoring sections (I and II) are arranged in front of and behind each monitoring station, numbered w-I and w-II, with $w = 1$–6. With the mining of the working face, the change of roadway floor deformation is shown in Fig. 19.
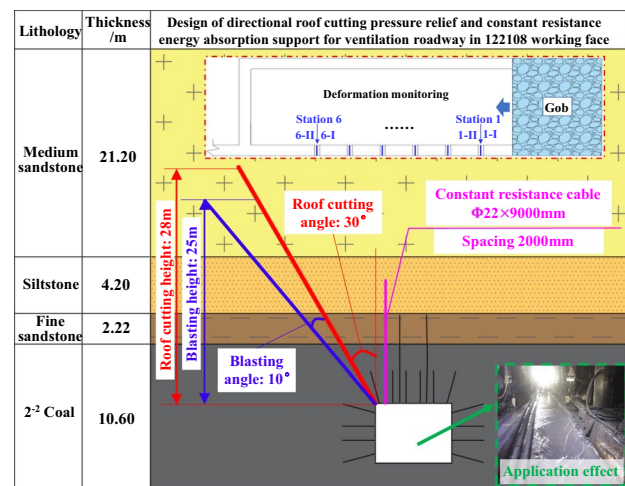

Fig. 18 Pressure relief parameters and reinforcement design

1. The average deformation of each monitoring section within 100 m of the mining face is 201.8 mm, which is 74.8% lower than the field actual deformation. This suggests that the comprehensive control method of directional roof cutting combined with strengthen blasting and energy-absorbing reinforcement is effective in ground control.

2. The floor deformation at the same position of the physical model in the previous section is 4.01 mm, which is converted into the field actual deformation of 240.6 mm by the geometric similarity scale of 1:60. The field measured result is slightly smaller than the physical model result, and the difference between the two is 16.13%, which verifies the rationality and effectiveness of the physical model result.

5.2.2 Stress Analysis of the Roadway Reinforcement

As the working face is being mined, the stress of the advanced reinforcement at the #122108 working face in the ventilation roadway is monitored in real time. Figure 20 shows the stress evolution of the advanced reinforcement along with the mining of the working face.

It can be seen from Fig. 20 that the stress of the roadway after directional roof cutting and strengthen blasting exhibits a stepwise descending trend.

1. Without blasting, the peak stress of the reinforcing system reaches 40 MPa, and the average stress is 27.1 MPa.

2. When the reinforcing system enters the test section from the start of blasting, the peak stress of the reinforcing system in the roadway decreases to 36.1 MPa, 8.25%
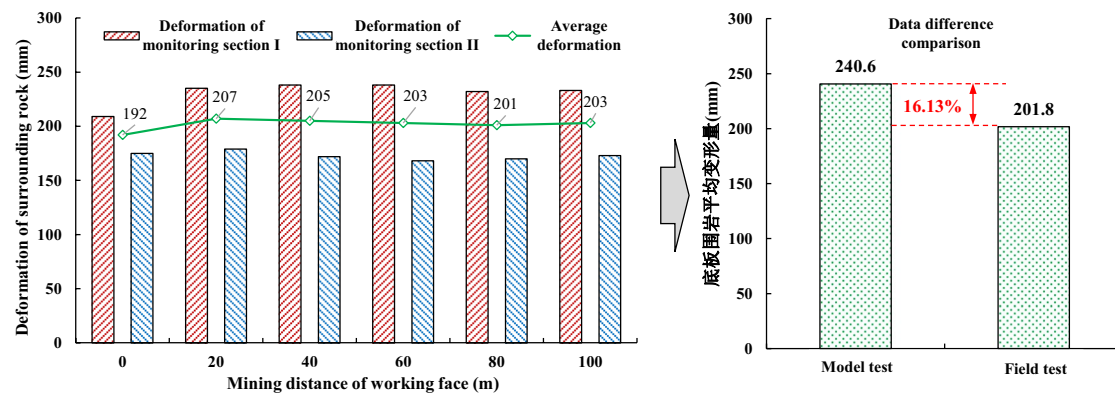
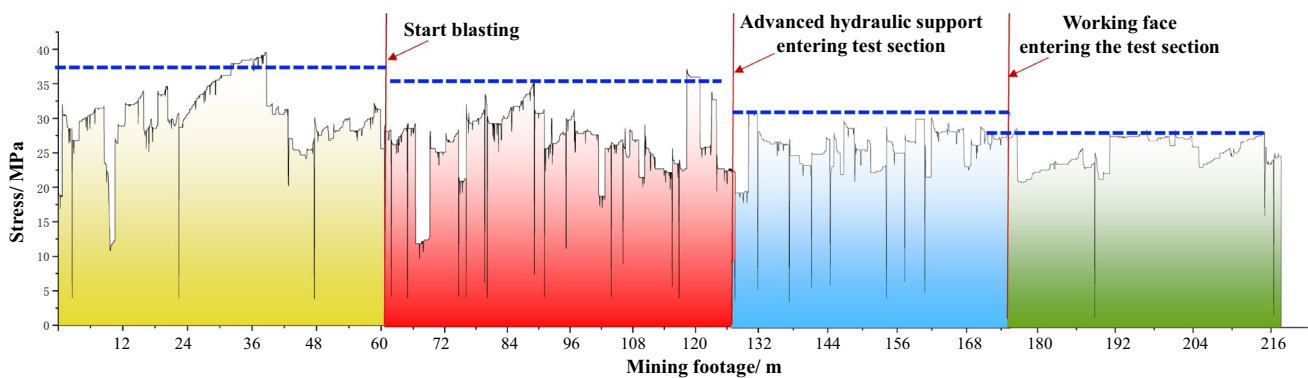**Fig. 19** Deformation variation of the roadway floor

Fig. 20 Stress evolution of the roadway ahead of the working face

less than that without blasting, and the average stress is 26.6 MPa, 1.84% less than that without blasting.

3. Between the reinforcing system enters the test section and the working face enters the test section, the peak stress decreases to 32.9 MPa, 17.75% less than that without blasting.

4. After the working face enters the test section, the peak stress of the reinforcing system in the roadway decreases to 28.9 MPa, 27.75% less than that without blasting, and the maximum reduction is 11.1 MPa.

It can be seen from the stress changes of the reinforcing system in the four stages described above that the stress decreases continuously with the mining of the working face after the comprehensive control method of directional roof cutting in combination with strengthen blasting and energy-absorbing reinforcement is implemented.

6 Conclusions

1. We proposed an integrated ground control method of roof cutting pressure relief and energy-absorbing reinforcement to tackle ground control challenges in extra-thick coal seams with extra-thick hard roof. Through directional roof cutting to cut off the stress transfer path between the roadway and the gob roof, the impact of hard roof collapse is reduced by strengthen blasting, and the constant-resistance energy-absorbing anchor cables are used to ensure the safety and stability of the roadway.

2. We conducted numerical simulations on different pressure relief parameters for roadway with thick hard roof. We analyzed the impacts of directional cutting and strengthen blasting parameters and examined three-dimensional stress evolution of the surrounding rock of the roadway. The advantages of roof cutting pressure relief and energy-absorbing reinforcement in the stability of the roadway are verified.

3. The model comparison test of pressure relief and energy absorption control of thick and hard roof roadway was carried out, and the difference of stress and control effect of roadway surrounding rock before and after the safety control method of roof cutting pressure relief and energy absorption support was obtained. Using the new ground control method, the average stress of the surrounding rock is reduced by 40.1%, the maximum deformation is reduced by 74.8%. The control mechanism of roof cutting pressure relief and support energy absorption in roadway with thick hard roof is clarified.

4. We carried out a field design and application of the new method based on the laboratory experimental results. Field monitored data shows that the average deformation of the roadway floor with the new control method is 201.8 mm, which is 66.37% less than that of the roadway without using the method, and the peak stress of the reinforcing system is 27.75% less than that without using the method. The fidelity of the physical model test data and the rationality of the design method of pressure relief reinforcing parameters are verified.

References

Bin Y (2016) Behaviors of overlying strata in extra-thick coal seams using top-coal caving method. J Rock Mech Geotech 8(02):238–247

Chen Y, Ma SQ, Yu Y (2017) Stability control of underground roadways subjected to stresses caused by extraction of a 10-m-thick coal seam: a case study. Rock Mech Rock Eng 50(09):2511–2520

Gao K, Liu ZG, Liu J, Deng DS, Gao XY, Kang Y, Huang KF (2013) Application of deep borehole blasting to gob-side entry retaining forced roof caving in hard and compound roof deep well. Chin J Rock Mech Eng 32(08):1588–1594

Gong S, Tan Y, Liu YP, Zhu D, Yu Y (2021) Application of presplitting blasting technology in surrounding rock control of gob-side entry retaining with hard roof: a case study. Adv Mater Sci Eng 2021:1318975

He MC, Gong WL, Wang J, Qi P, Tao ZG, Du S, Peng YY (2014) Development of a novel energy-absorbing bolt with extraordinarily large elongation and constant resistance. Int J Rock Mech Min 67:29–42

He MC, Zhu GL, Guo ZB (2015) Longwall mining cutting cantilever beam theory and 110 mining method in China The third mining science innovation. J Rock Mech Geotech 7(05):483–492

He MC, Gao YB, Yang J, Wang JW, Wang YJ, Zhu Z (2018) Engineering test of rapid mining, roof cutting and pressure relief in thick coal seam and self forming roadway without coal pillar. Geotech Mech 39(01):254–264

He MC, Wang Q, Wu QY (2021) Innovation and future of mining rock mechanics. J Rock Mech Geotech 13:1–21

Jiang B, Xin ZX, Zhang XF, Deng YS, Wang MZ, Li SD, Ren WT (2023) Mechanical properties and influence mechanism of confined concrete arches in high-stress tunnels. Int J Min Sci Technol. https://doi.org/10.1016/j.ijmst.2023.03.008

Kang HP, Wang GF, Jiang PF, Wang JC, Zhang N, Jing HW, Huang BX, Yang BG, Guan XM, Wang ZG (2018) Conception for strata control and intelligent mining technology in deep coal mines with depth more than 1000m. J Chin Coal Soci 43(07):1789–1800

Li XW, Aziz N, Mirzaghorbanali A, Nemcik J (2016) Behavior of fiber glass bolts, rock bolts and cable bolts in shear. Rock Mech Rock Eng 49(07):2723–2735

Li B, Xu NW, Xiao PW, Xia Y, Zhou X, Gu GK, Yang XG (2023) Microseismic monitoring and forecasting for dynamic disasters of underground engineering in hydropower projects. J Rock Mech Geotech. https://doi.org/10.1016/j.jrmge.2022.10.017

Mao HY, Xu NW, Li X, Li B, Xiao PW, Li YH, Li P (2023) Analysis of rockburst mechanism and warning based on microseismic moment tensors and dynamic Bayesian networks. J Rock Mech Geotech. https://doi.org/10.1016/j.jrmge.2022.12.005

Wang W, Cheng YP, Wang HF, Liu HY, Wang L, Li W, Jiang JY (2015) Fracture failure analysis of hard-thick sandstone roof and its controlling effect on gas emission in underground ultra-thick coal extraction. Eng Fail Anal 54:150–162

Wang Q, Jiang ZH, Jiang B, Gao HK, Huang YB, Zhang P (2020a) Research on an automatic roadway formation method in deep mining areas by roof cutting with high-strength bolt-grouting. Int J Rock Mech Min 128:104264

Wang Q, Qin Q, Jiang B, Jiang ZH, He MC, Li SC, Wang Y (2020b) Geomechanics model test research on automatically formed roadway by roof cutting and pressure releasing. Int J Rock Mech Min 135:104506

Wang Q, Gao HK, Jiang B, Li SC, He MC, Qin Q (2021a) In-situ test and bolt-grouting design evaluation method of underground engineering based on digital drilling. Int J Rock Mech Min 138:104575

Wang Q, He MC, Li SC, Jiang ZH, Wang Y, Qin Q, Jiang B (2021b) Comparative study of model tests on automatically formed roadway and gob-side entry driving in deep coal mines. Int J Min Sci Techno 31(04):591–601

Wang Q, Xu S, He MC, Jiang B, Wei HY, Wang Y (2022a) Dynamic mechanical characteristics and application of constant resistance energy-absorbing supporting material. Int J Min Sci Technol 32:447–458

Wang Q, Xu S, Xin ZX, He MC, Wei HY, Jiang B (2022b) Mechanical properties and field application of constant resistance energy-absorbing anchor cable. Tunn Undergr Sp Tech 125:104526

Wang Q, Wang Y, He MC, Li SC, Jiang ZH, Jiang B, Xu S, Wei HY (2022c) Experimental study on the mechanism of pressure releasing control in deep coal mine roadways located in faulted zone. Geomech Geophys Geo 8(02):1–24

Wei WJ, Yang SL, Li M, Zhang JW, Wei CB (2022) Motion mechanisms for top coal and gangue blocks in longwall top coal caving (LTCC) with an extra-thick seam. Rock Mech Rock Eng 55(08):5107–5121

Wojtecki L, Iwaszenko S, Apel DB, Bukowska M, Makowka J (2022) Use of machine learning algorithms to assess the state of rockburst

hazard in underground coal mine openings. J Rock Mech Geotech 14(03):703–713

Xiong ZQ, He HJ (2006) Numerical simulation of rock burst stress state and its control by stress-relief. J Min & Safe Eng 04:489–493

Yang JZ, Zheng KG (2020) The mechanism of overburden dynamic disasters and its control technology in top-coal caving in the mining of thick coal seams. J Min Safe Eng 37(04):750–758

Zhao T, Liu CY, Yetilmezsoy K, Zhang BS, Zhang S (2017) Fractural structure of thick hard roof stratum using long beam theory and numerical modeling. Environ Earth Sci 76(21):751

Zhu GA, Jiang QP, Wu YP, Dou LM, Lin ZQ, Liu HY (2021) Numerical inversion of dynamic behavior of fault slip instability induced by stress waves. J Min Safe Eng 38(02):370–379